The process of making a pico satellite

Reza Ali pour
[1]Researcher

Abstract

The subject of this paper is the fabrication process of a pico-satellite mounted in a 345-liter polyethylene terephthalate bottle that was assembled and tested during the 6th Can Sat Leader training program at Hokkaido University, Japan. This mission is to measure physical variables. Like temperature and humidity, which are designed using electronic sensors, the purpose of this article is to explain the manufacturing process and how to use the pico satellite, so that students can familiarize themselves with its manufacturing process during their studies in educational centers. The result shows that the system is equipped with temperature and humidity sensors, and consists of an array of helium balloons that are attached to pulleys on the ground. And it is placed at different heights. Each balloon carries a pico-satellite and temporarily remains at a fixed altitude while data is transmitted to a distant ground station. Once each pico mast has completed its mission, it is released from the balloon and recovered at the rendezvous point.

Keywords: Pico satellite, satellite construction, weather monitoring.

[1] Reza Ali pour, telecommunication systems specialist, Islamic Republic of Iran

Introduction

subject:

The subject of this paper is the fabrication process of a pico -satellite mounted in a 345 m L polyethylene terephthalate (PET) bottle that was assembled and tested during the 6th Can Sat Leader Training Program (CLTP-6) at Hokkaido University - Japan this summer. and completed in 2015, it should be noted that the Pico satellite at the Uematsu Electric Co. facility. Ltd in Akabira - Japan has launched a paper model, a rocket that reaches an approximate height of 100 meters. The mission is designed to measure physical variables such as temperature and humidity using electronic sensors. During the flight, we observed that the temperature inside the rocket is 0.5 ◦ C higher than the ambient temperature. We recorded a measured humidity difference of ~5% between the maximum altitude and the landing point. A flight pattern with GPS coordinates was shown to the aircraft covering an area of 50 x 50 meters. [1].

In the following:

In the continuation of this article, it will be explained as follows. definitions, Description and assembly of the picosatellite, Test and results, Launch and results, Applications, Summary of findings, Conclusions

definitions

Emerging technologies used for space education have been growing rapidly since the last decade and small satellites are playing an important role in academies around the world In particular, the expansion and knowledge of Can Sat pico Mas satellites has opened up a new branch in space education programs [2].as it provides a context and motivational context for students to start or continue their studies [3]. In addition, it can be shown that the A pico satellite is a powerful tool if combined with scientific devices to achieve professional experiments [4] In this paper, we describe the results and process of assembling and testing a pico-satellite mounted in a 345 mL polyethylene terephthalate (PET) bottle. The experiments were conducted in the summer of 2015 during the 6th Can Sat Leadership Training Program [5]. which was held at Hokkaido University-Japan in collaboration with the Space University Engineering Consortium [6].

Description of pico satellite assembly

✓ The Pico satellite consists of six subsystems, each of which has a printed circuit board (PCB), on which all the electronic components are soldered and assembled as follows:

(a) Power subsystem. It uses a 9V alkaline battery (dry cells) that acts as a power supply for the entire system

(b) Communication subsystem. It consists of a transmission module with an X Bee Pro-Z net antenna, which uses the wireless communication protocol ZigBee (IEEE802.15.4) and a receiving module, which consists of a USB board Mod-Pro with an X Bee (similar to the previous one), to a computer The laptop is connected, thus forming a ground station.

(c) Global Positioning System (GPS). It uses GPS module GMS6-CR6 (9600 bps). (d) Computer subsystem. Consists of

✓ A PIC16 8-bit RISC microcontroller, with 24LC1025-I/P 1MB serial EEPROM memory. This component of I 2 C programming language. (e) Micro camera. It uses a concept Micro 808 Car Key camera, integrated on the PCB, to take pictures with a resolution of 720 x 480 pixels. temperature), pressure sensor MPL115A2, gyroscope sensor ENC-03R and accelerometer sensor AS-3ACC-3. Six PCBs with some soldered electronic components are shown in Figure 1.

✓ All the PCBs are connected to each other with pin connectors and connected instead of electrical wires to match the integrity in a cal structure cylinder, as shown in the picture in figure 2.

✓ In this image, the structure is compared in size to a PET bottle. In this same image, we can also see the page on the manual assembly. The complete device inserted into the bottle is shown in Figure 3.

It should be considered that a mechanism must be implemented to achieve a slow landing. For this purpose, a system consisting of three deployable parachutes was implemented outside the bottle. Each

parachute was constructed with plastic bags with a hexagonal geometry carved into a 35-cm-diameter circle and tightened with 6 25-cm-long strings on each edge. A 6 cm circular hole was drilled in the center of each parachute to provide vertical stability during landing, and finally, each parachute was attached every 120 ◦ around the bottle.

To check the deployment of the parachute and confirm the transmission of data by telemetry, the Pico satellite was launched manually from the window of a building 10 meters high during the landing, the total mass m = 0.18 kg of the Pico satellite and the parachute force equivalent to its own weight with friction k. proportional to the square of the speed.

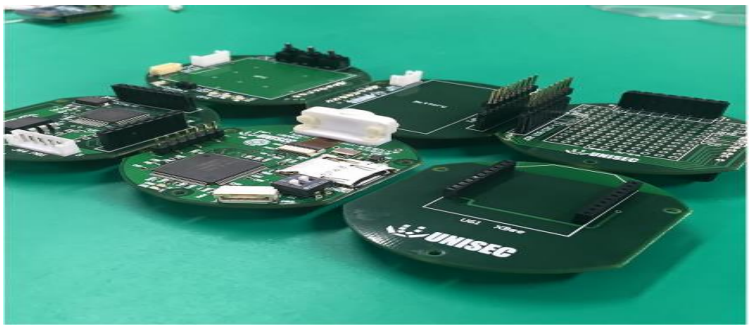

Figure 1. Six PCBs (one for each subsystem), with some electronics soldered on

For this particular case, k = 1.94. We considered enviromental conditions so the air density ρ = 1.1647 is obtained, estimated at T = 29 ◦ C, P = 1019 hPa, relative humidity 58%, and dew point 19.91 ◦ C. In these conditions the drag force D according to The following equations produce a descent velocity v e equal to 2.7 m/s.

$$D \frac{1}{2} p^C D^A v^2 \qquad (1)$$

Figure 2. Comparison of the size of the assembly with a PET bottle and the cover page of the assembly manual.

Fig. 3. Full system, introduced into a PET-bottle.

$$v_e = \sqrt{\frac{2W_t}{S_o C_D \rho}} \quad (2)$$

where C D = (D/Aρ) = 1.75, is the drag coefficient: A, transverse area of the object; v is the speed. W t is the total weight; S 0 is the level of the parachute. While to determine the speed at any moment after the parachute Establishment, we used where t is the time in seconds and g is the gravity.

$$v(t) = \left(\frac{mg}{k}\right)(1 - e^{\frac{k}{m}t}) \quad (3)$$

Test and results

To verify the functionality and performance of the system integration, we conducted two tests under extreme conditions:

(a) thermal vacuum test and

(b) vibration test.

Thermal vacuum testing is useful for observing the thermal equilibrium state and performance of an electronic combination to check a thermal design, surface material properties, and to reveal potential errors in a program system [7]. For our purposes, we performed the experiment only by introducing the integrated structure. The interior of the the rmotron device model S-8-8200 (TM THERMOTRON Industries Ltd.), as shown in Figure 4. We used a thermal cycler from 0 ◦ C to 40 ◦ C initialized at room temperature (25 ◦ C) to complete a period of approximately 2 h. During this time, we observed a break in communication between the system and the ground station. This happened after 45 minutes from the starting point. This may be due to the reduced performance of the alkaline battery at low temperatures, so the discharge time becomes faster. The results of the thermal cycle are shown in Figure 5. Here, we can understand that the estimated cycle has two periods of maximum and two periods of minimum stabilized temperature: respectively at 0 ◦ C and at 40 ◦ C. Such periods last approximately 15 minutes.

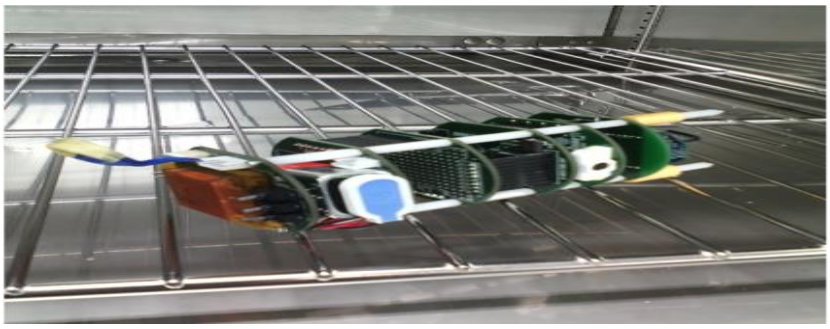

Fig. 4. Assembled structure, ready for starting a vacuum thermal cycle

Vibration tests are important to confirm that the integrated system can withstand the vibration of the environment during launch and the moment of separation With the rocket, in this case, the shock and random testing required to check the tolerance to the launch vibration and to the load acceleration range, for our purposes, we introduced the vibration test with our complete system.to a polyethylene tube, which runs in a mechanism on a metal platform that is screwed to the generator vibrator model 916-AW/LA which in turn is combined with a vibration[9].

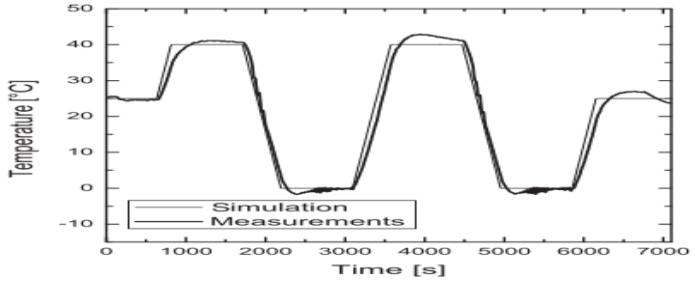

Fig. 5. Results of the thermal vacuum test.

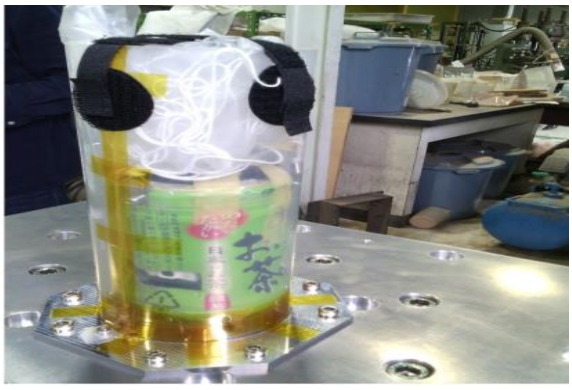

Fig. 6. Full system mounted in the setup for the vibration test.

Test system model F-16000BDH/LA16AW (TM EMIC Co., Japan). A picture of the setup is shown in Figure 6, and the results are shown in Figure 10-7. In Figure 7, the random histogram shows the acceleration over a period of 0.2 seconds. Figure 8 shows the power spectrum density (PSD). Where the continuous thin line shows the expected value and the dark line shows the measurements. Is. Dotted lines and dashed lines show the tolerances and limits, which show that we see the shock in Figure 9, warning and abortion, respectively. [10],[11].

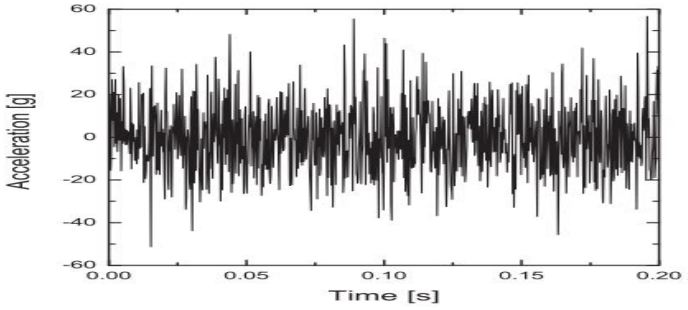

Figure 7. Random acceleration history.

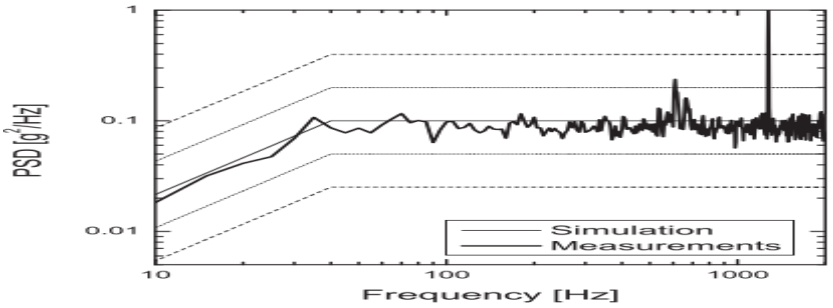

Fig. 8. Power spectrum density.

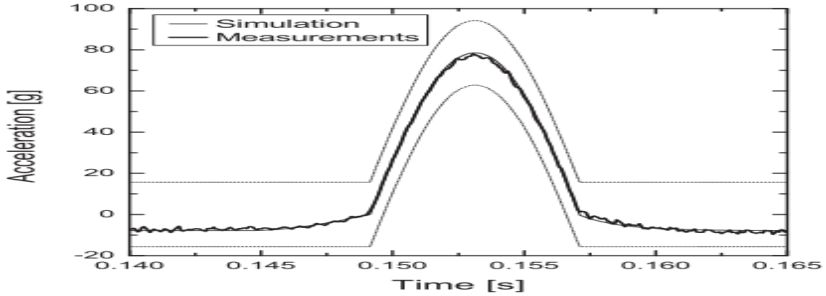

Fig. 9. Shock history of acceleration.

Acceleration history, where the thin line is the expected value, the dashed line is the measurement, and the dotted line is the tolerance. In Figure 10, Fast Fourier Transform (FFT) is used to obtain the shock spectrum. A summary of the parameters used for the vibration test is shown in Table 1, the directions considered for the longitudinal axis of the missile [12].

Table 1Summary of the vibration test.

Type of vibration	Direction[Z-axis] [Z-axis]	Freq. [Hz]	Accel.[G]	Duration [s]
Random	+Z	10	7.88	0.2
PSD	+Z	5-5000	1.4	7
Shock	+Z	5-5000	4.0	0.2

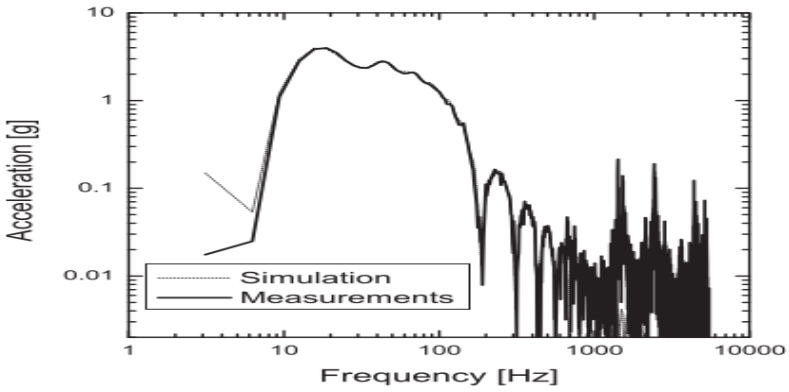

Figure 10. FFT shock spectrum.

Launch and results

The launch was conducted in the facilities of UEMATSU

Electric Co. Ltd. in Akabira-Japan, where the paper craft model rocket was designed and supported. This rocket has a height of90 cm, with a cylindrical body of 7 cm of diameter, and a mass of0.1 kg. It uses a cartridge model rocket engine, model D12-3 for a single stage (TM ESTES Industries Penrose, Co. USA). The mass of the cartridge is 0.025 kg. Therefore, the full load in cluding the 0.18 kg of the pico-satellite was 0.305 kg. This caused throcket to only reach a height of approximately 100 m. A picture of the rocket compared in size with the pico-satellite is shown in Figure 11. In this picture, we can see the instant when the rocket goes up. There are no verification results during launch to be compared with those of the vibration tests because the paper model rocket was built manually and did not contain electronic plat-forms to install vibration sensors or telemetry. This rocket was considered as a launch vehicle only. However, we assumed that each part of the pico-satellite was subjected to the maximum mechanical stress mainly at the beginning of launch and at the shock produced in the instant of separation. We also assumed that there were aerodynamic loads exerted to the pico-satellite during the launch stages such as longitudinal acceleration, sinusoidal vibrations produced by the combustion engine and natural movement of the launch vehicle, as well as random vibrations generated by acoustic noise of the combustion engine. For our purposes in both cases: tests and launch, the telemetry worked successfully without anomalies, demonstrating the reliability of the entire system. Figure 12 shows the instant of separation and the successful deployment of the parachutes. The pictures in Figure 13 were taken with the micro-camera during the descent. Note that the site is a rural-urban zone surrounded by grass and trees, while the launching point is a dry and large area made of asphalt.[12].

During the ascent and descent of the pico satellite, the sensor measured the temperature and humidity every second, and the data was transmitted by telemetry to the ground station, which was connected to a laptop computer, then the data was plotted. The results of the measurements are shown in Figures 14-16. In these figures, we can see that the flight time was about 250 seconds. [12].

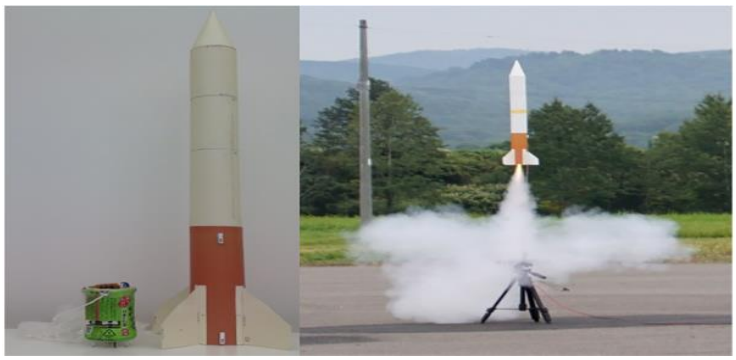

Figure 11. Pico satellite before and during launch.

Figure 12. Separation from the rocket and successful parachute deployment.

Fig. 13. Pictures taken with the micro-camera during the descent.

From the launch point to the landing point. It should be noted that the first part of the plans (about 200 seconds) includes both the preparation time on the platform and the time to climb to the maximum height. After that, the curves suddenly dropped and changed due to separation from the rocket. Figure 14 shows a temperature drop of ∼0.5 ◦ C, which means that the interior of the rocket is warmer than the environment. This temperature difference may be caused by gas production. - Entered by the engine during propulsion. On the other hand, we observed that the humidity decreased by about 5% from the maximum height to the landing point. It should be considered that the weather conditions were cloudy. Although even the distance from the ground to the maximum height was relatively short, but

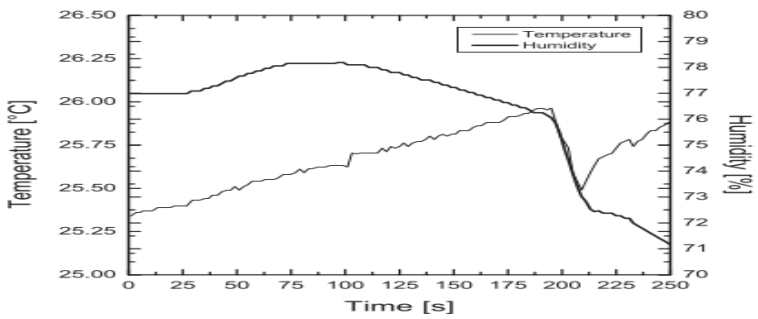

Figure 14. Temperature and humidity, measured during ascent and descent of the Pico satellite.

could be possible to measure this humidity difference because the characteristics of the zone indicate that there may be different conditions between the wet grass and trees with respect to the dry asphalt area, where the landing point occurred. In order to know an approximation of the real area where the measurements were taken, the flight pattern was projected to a plane, as depicted in Figure 17. Here, the frame is scaled [12].

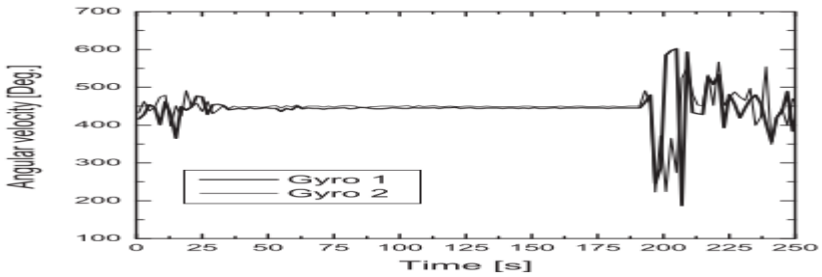

Fig. 15. Rotational movements, measured with the gyroscope.

by the coordinates measured with the GPS. Hence, an estimated area can be calculated by using the polygonal of the projected pattern. According to the dimensions of UEMATSU facilities, the asphalt covers an area of around 50 m × 50 m. finally, the pico-satellite was recovered at its landing point and we confirmed that no damage occurred during the impact, up to then, the system was switched off. Figure 18 shows its physical stage, after finishing the mission [12].

Applications

An astronomical observatory needs constant monitoring of weather conditions, especially before the start of operations to observe the sky, although these sites have their own meteorological station and review of meteorological data from the satellite system.

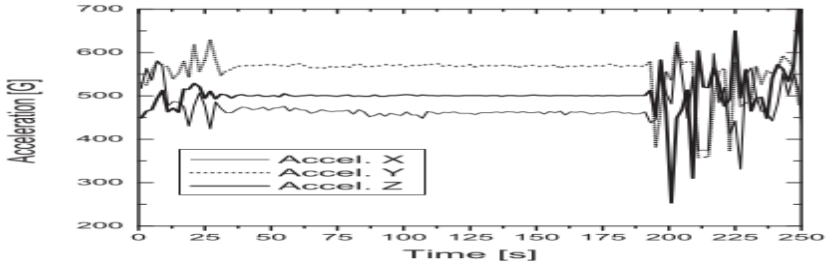

Fig. 16. Change of acceleration, measured in the xyz-axis.

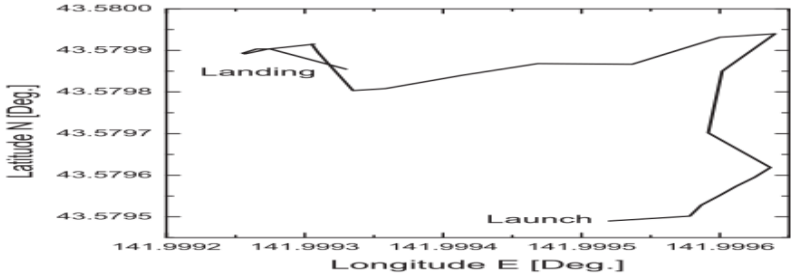

Figure 17. Flight pattern of Pico satellite, launched on an airplane.

teems, a climate monitoring in small areas of the site turns out to be complementary if the measurements are conducted at alti-tudes below 1 km. Particularly, the facilities of the (OA-UANL) are still under construction [8]. therefore, making decisions about the best place in the site to install a professional telescope requires as much climatic information as possible. Since the beginning of 2012, this site has

been monitored using only a weather station (Davis Instrument 6162C) and three compact sensors (Spectrum Technologies Inc. B100 Button Logger) placed at ground level [12].

Figure 18. Pico satellite, recovered at the landing point.

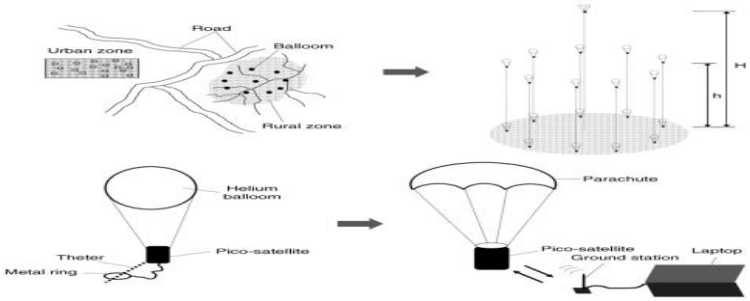

Figure 19. Schematic for weather monitoring in rural and urban areas, using geometric configuration of pico satellites at different altitudes below 1 km.

For our purposes, we will use ten equipped picosatellites with temperature and humidity sensors and thus forming a set Helium balloon tied to pulleys on the ground are placed at different heights. Each balloon carries a pico-satellite and remains at a fixed altitude temporarily while data is transmitted to a mobile ground station. Once each pico-satellite has completed its mission, it is released from the balloon and recovered at the docking point. A schematic diagram of the method is shown in Figure 19. Note that this method can also be used in urban areas to approach different monitoring studies by changing the configuration geometry and the type of sensors. [12].

The results

Conclusion and discussion

The results and findings of this paper indicate that this research is the process of making a pico satellite installed in a 345liter polyethylene terephthalate (PET)bottle in the 6th Can Sat Leader Training Program (CLTP-6) at Hokkaido University. - Assembled and tested in Japan. This shows that ten Pikoma satellites have been used for their purposes. This system is equipped with temperature and humidity sensors, and as a result, a set of helium balloons are connected to the reels on the ground. are located at different heights. Each balloon carries a pico-satellite and temporarily remains at a fixed altitude while data is transmitted to a distant ground station. Once each picoma satellite has completed its mission, it is released from the balloon and recovered at the rendezvous point. It should be noted that this method can also be used in urban areas by changing the geometry of the configuration and the type of sensors to approach different monitoring studies. Therefore, according to the national goals of innovation and research investment in universities at the postgraduate level, it can be shown that they can be a powerful tool and can be used with scientific tools to conduct experiments and improvements. It is worth mentioning that my findings are the same as the findings of the researchers of this article and there is no conflict.

Proposa

With innovation and research investment in specialized universities and at the level of supplementary education in different countries, it can be shown that this project can be a powerful tool and can be used in cooperation with scientific, educational and research centers to test and improve this system.

References

[1]. Thakker, P., & Shiroma, W. A. (2010). Emergence of pico- and nanosatellites for atmospheric research and technology testing. Virginia: American Institute of Aeronautics and Astronautics Inc.

[2]. Nakasuka, S. (2013). CanSat Lecture CanSat Lecture – Its edu-cational significance.. Available from: [2]

[3]. Ayala, S., Colin, A., González, A. R., Rivas, R., Mona, J., Avilés, A., et al. (2016).

[4]. Colin, A. (2015). The Can Sat technology for climate Monitoring in small regions at altitudes below 1 km. In IAA Climate Change & Disaster Management Conference.

[5]. CLTP-6. (2015). 6th Can Sat Leader Training Program. Available from:[3]

[6]. UNISEC. (2015). University space engineering consortium. Available from[4]

[7]. Masui, H., Hatamura, T., & Cho, M. (2013). Testing of micro/nano satellites and their on-orbit performance. In UT-USA, 27th Annual AIAA/USU Conference on Small Satellites.

[8]. Colin, A., Ayala, S., Vázquez, R., Olguín, L., Adame, L., Avilés, A., et al. (2016). 91The astronomical observatory of UANL, Monterrey, Mexico. 20.DA10: Research and teaching in astrophysics in Guanaju at o. In Proceedings of a Conference Held at Guanajuato, GTO.

[9]. UNISEC-Mexico. (2015). University space engineering consortium, chapter México. Available from[5]

[10]. Walker, R., Galeone, P., Page, H., Castro, A., Emma, F., Callens, N., et al. (2010). ESA hands-on space education project activities for university students: Attracting and training the next generation of space en gineers. In Paper presented at the 2010 IEEE Education Engineering Conference, EDUCON2010, 1699–1708.

[11]. Wang, T., & V and eberg, R. (2009). Norwegian Can Sat competition pilot. Available from:[6]

[12]. Angel Colin, (2017), A pico-satellite assembled and tested during the 6th Can Sat Leader Training Pro gram, University of Nuevo León - Faculty of Physics and Mathematics, Av. s/n, (1), 9(83-91).[7]

[2] http://www.unisec-global.org/pdf/1/2 Nakasuka.pdf Accessed January 2015

[3] http://cltp.info/cltp6.html Accessed December 2015

[4] http://www.unisec-global.org/ Accessed December 2015

[5] http://www.unisec.mx/#top Accessed December2016

[6] https://www.redalyc.org/journal/474/47450521010/html/

[7] https://jart.icat.unam.mx/index.php/jart/article/view/10/10